This is the accepted manuscript made available via CHORUS. The article has been published as:

Top Quark Mass Calibration for Monte Carlo Event Generators

Mathias Butenschoen, Bahman Dehnadi, André H. Hoang, Vicent Mateu, Moritz Preisser, and Iain W. Stewart

Phys. Rev. Lett. **117**, 232001 — Published 29 November 2016

DOI: 10.1103/PhysRevLett.117.232001

IFT-UAM/CSIC-16-069, FTUAM-16-28, MIT-CTP 4820, UWTHPH 2016-13, DESY 16-150

Top Quark Mass Calibration for Monte Carlo Event Generators

Mathias Butenschoen,[1] Bahman Dehnadi,[2] André H. Hoang,[2,3]
Vicent Mateu,[4] Moritz Preisser,[2] and Iain W. Stewart[5]

[1] *II. Institut für Theoretische Physik, Universität Hamburg, Luruper Chaussee 149, D-22761 Hamburg, Germany*
[2] *University of Vienna, Faculty of Physics, Boltzmanngasse 5, A-1090 Wien, Austria*
[3] *Erwin Schrödinger International Institute for Mathematical Physics, University of Vienna, Boltzmanngasse 9, A-1090 Wien, Austria*
[4] *Departamento de Física Teórica and Instituto de Física Teórica, IFT-UAM/CSIC, Universidad Autónoma de Madrid, Cantoblanco, 28049, Madrid, Spain*
[5] *Center for Theoretical Physics, Massachusetts Institute of Technology, Cambridge, MA 02139, USA*

The most precise top quark mass measurements use kinematic reconstruction methods, determining the top mass parameter of a Monte Carlo event generator, $m_t^{\rm MC}$. Due to hadronization and parton shower dynamics, relating $m_t^{\rm MC}$ to a field theory mass is difficult. We present a calibration procedure to determine this relation using hadron level QCD predictions for observables with kinematic mass sensitivity. Fitting e^+e^- 2-Jettiness calculations at NLL/NNLL order to Pythia 8.205, $m_t^{\rm MC}$ differs from the pole mass by 900/600 MeV, and agrees with the MSR mass within uncertainties, $m_t^{\rm MC} \simeq m_{t,1\,\rm GeV}^{\rm MSR}$.

PACS numbers: 12.38.Bx, 12.38.Cy, 12.39.St, 24.85.+p

Making more precise measurements of Standard Model parameters is a major aim of the collider physics program. The determination of the top quark mass is important due to its influence on many quantitative and conceptual aspects for the Standard Model and beyond. The most precise determinations to date include the combined result from the Tevatron $m_t = 174.34(64)\,\text{GeV}$ [1], CMS Run-I $m_t = 172.44(49)\,\text{GeV}$ [2], and ATLAS Run-I $m_t = 172.84(70)\,\text{GeV}$ [3].

The highest precision measurements are based on direct reconstruction methods exploiting kinematic properties related to the top quark mass, and are based on multivariate fits that depend on a maximum amount of information on the top decay final states. This includes template and matrix element fits for distributions such as the measured invariant mass. These observables are highly differential, depending on experimental cuts and jet dynamics. Multipurpose Monte Carlo (MC) event generators are employed to do the analysis, and the results are influenced by both perturbative and non-perturbative QCD effects. Thus the measured mass is the top mass parameter $m_t^{\rm MC}$ contained in the particular MC event generator. Its interpretation may also depend in part on the MC tuning and the observables used in the analysis.

The systematic uncertainties from MC modeling are a dominant uncertainty in the above measurements, but do not address how $m_t^{\rm MC}$ is related to a mass parameter defined precisely in quantum field theory that can be globally used for higher order predictions. The relation is nontrivial because it requires an understanding of the interplay between the partonic components of the MC generator (hard matrix elements and parton shower) and the hadronization model. In the context of top quark mass determinations it is often assumed that MC generators should be considered as models whose partonic components and hadronization models are, through the tuning procedure, capable of describing experimental data to a precision that is higher than that of their partonic input.

In the past $m_t^{\rm MC}$ has been frequently identified with the pole mass. This is compatible with parton-shower implementations for massive quarks, but a direct identification is disfavored because of sensitivity to non-perturbative effects from below the MC shower cutoff $\Lambda_c \sim 1\,\text{GeV}$. Also, the pole mass has an $\mathcal{O}(\Lambda_{\rm QCD})$ renormalon ambiguity, while $m_t^{\rm MC}$ does not (since partonic information is not employed below Λ_c). It has been argued [4, 5] that $m_t^{\rm MC}$ has a closer relation to the MSR mass $m_t^{\rm MSR}(R \approx \Lambda_c)$, where the scale R defining this scheme is close to Λ_c. The MSR mass $m_t^{\rm MSR}(R)$ [6] applies the pole mass subtraction for momentum fluctuations from above R and also does not suffer from the renormalon ambiguity.

For a given MC generator, $m_t^{\rm MC}$ can be calibrated into a field theory mass scheme through a fit of MC predictions to *hadron level* QCD computations for observables closely related to the distributions that enter the experimental analyses. In this letter we provide a precise quantitative study on the interpretation of $m_t^{\rm MC}$ in terms of the MSR and pole mass schemes based on a hadron level prediction for the variable τ_2 for the production of a boosted top-antitop quark pair in e^+e^- annihilation. It is defined as:

$$\tau_2 = 1 - \max_{\vec{n}_t} \frac{\sum_i |\vec{n}_t \cdot \vec{p}_i|}{Q}\,, \tag{1}$$

where the sum is over the 3-momenta of all final state particles, the maximum defines the thrust axis $\vec{n}_{\rm t}$ and Q is the center of mass energy. In Refs. [7, 8] a factorization theorem has been proven for boosted top quarks, yield-

ing hadron level predictions for τ_2, which we refer to as 2-Jettiness [9]. For unstable top quarks it is very close to thrust which has the sum of the 3-momenta magnitudes for final states instead of Q in Eq. (1). The τ_2 distribution has a distinguished peak very sensitive to the top mass, and is a delta function at $\tau_2^{\min}(m_t) = 1 - \sqrt{1-4m_t^2/Q^2}$ at tree level. The peak region is dominated by dijet events where the top quarks decay inside narrow back-to-back cones and τ_2 is directly related to the sum of the squared invariant masses $M_{a,b}^2$ in the two hemispheres defined by the thrust axis $\vec{n}_t$, $(\tau_2)_{\rm peak} \approx (M_a^2 + M_b^2)/Q^2$. Thus τ_2 in the peak region is an observable with kinematic top mass sensitivity, just like those that enter the top quark mass reconstruction methods. Thus the results of our calibration study should provide information relevant for the interpretation of these measurements.

2-Jettiness Distribution: The τ_2 distribution in the peak region for boosted top quarks has the basic form

$$\frac{\mathrm{d}\sigma}{\mathrm{d}\tau_2} = \int \mathrm{dk} \left(\frac{\mathrm{d}\hat\sigma_{\rm s}}{\mathrm{d}\tau_2} + \frac{\mathrm{d}\hat\sigma_{\rm ns}}{\mathrm{d}\tau_2}\right) \left(\tau_2 - \frac{\mathrm{k}}{\mathrm{Q}}\right) \mathrm{F}_{\tau_2}(\mathrm{k}) \Big[1 + \mathcal{O}\big(\tfrac{\Lambda_{\rm QCD}}{Q}, \tfrac{\Gamma_t}{m_t}\big)\Big], \tag{2}$$

where $\mathrm{d}\hat\sigma_{\rm s}/\mathrm{d}\tau_2$ contains the singular partonic QCD corrections $\alpha_s^j \, [\ln^k(\tau_2 - \tau_2^{\min})/(\tau_2 - \tau_2^{\min})]_+$ and $\alpha_s^j \, \delta(\tau_2 - \tau_2^{\min})$ in the dijet limit and $\mathrm{d}\hat\sigma_{\rm ns}/\mathrm{d}\tau_2$ stands for the remaining partonic nonsingular QCD corrections. The shape function F_{τ_2} describes the non-perturbative effects from wide-angle soft gluon radiation [10]. The singular partonic contribution obeys a factorization theorem

$$\begin{aligned}
\frac{\mathrm{d}\hat\sigma_{\rm s}}{\mathrm{d}\tau_2} &= H_Q^{(6)}(Q,\mu_Q) U_{H_Q}^{(6)}(Q,\mu_Q,\mu_m) H_m^{(6)}(Q,m_t,\mu_m) \\
&\times Q\, U_{H_m}^{(5)}\Big(\frac{Q}{m_t},\mu_m,\mu_B\Big) \int \mathrm{ds} \int \mathrm{dk}\, J_{B,\tau_2}^{(5)}\Big(\frac{s}{m_t},\mu_B,\Gamma_t,\delta m_t\Big) \\
&\times U_S^{(5)}(k,\mu_B,\mu_S) \hat S_{\tau_2}^{(5)}\Big(Q[\tau_2 - \tau_2^{\min}(m_t)] - \frac{s}{Q} - k, \mu_S\Big),
\end{aligned} \tag{3}$$

based on Soft-Collinear-Effective Theory [11–14], which separates the contributions from the hard interactions in the hard functions H_Q and H_m, the jet function J_{B,τ_2}, and the soft cross-talk between the top and antitop jets in the partonic soft function $\hat S_\tau$. The jet function J_{B,τ_2} is derived in boosted HQET [7] since the collinear top jet invariant mass in the peak region is very close to the top quark mass. It includes the collinear dynamics of the decaying top quarks and leading top finite-width effects. The various evolution factors U_X sum large logarithms.

Results for $\mathrm{d}\hat\sigma_{\rm s}/\mathrm{d}\tau_2$ with next-to-leading logarithmic resummation $+\,\mathcal{O}(\alpha_s)$ singular corrections (NLL + NLO) can be found in Ref. [8], with the addition of the virtual top quark contribution and rapidity logarithms in H_m and U_{H_m} from Ref. [15]. The N^{2}LL evolution in U_{H_Q} and U_S is known from the massless quark case, and is consistent with the direct $\mathcal{O}(\alpha_s^2)$ calculation of the J_{B,τ_2} anomalous dimension [16]. We implemented all the N^{2}LL order ingredients for the proper treatment of the flavor number dependence [superscript (6) for including top as dynamic quark versus superscript (5) for excluding the top] in the RG evolution [17, 18]. We also include the $\mathcal{O}(\alpha_s)$ nonsingular corrections $\mathrm{d}\hat\sigma_{\rm ns}/\mathrm{d}\tau_2$ [19].

For the shape function F_{τ_2} we use the convergent basis functions introduced in Ref. [20] truncated to 4 elements (where the 4-th element is already numerically irrelevant). These elements determine moments of the shape function Ω_i [21, 22], which are the parameters that can also be fit together with α_s in event-shape analyses [21–28]. The leading power correction Ω_1 is defined in the R-gap scheme such that it cancels an $\mathcal{O}(\Lambda_{\rm QCD})$ renormalon present in $\hat S_{\tau_2}$ [29]. This is achieved through an appropriate subtraction series $\delta(R_S, \mu_S)$ [30] which induces both R_S and μ_S dependence in Ω_1. We quote results for Ω_1 at the reference scales $\mu_S = R_S = 2\,\mathrm{GeV}$. The evolution of Ω_1 with R_S is described by R-evolution [6, 31].

Eq. (3) is written in terms of a generic mass scheme m_t, with $\delta m_t = m_t^{\rm pole} - m_t$ in $J_{B,\tau_2}^{(5)}$ controlling the dominant sensitivity to the mass scheme. In the pole mass scheme $\delta m_t = 0$. Using renormalon-free schemes, the $\overline{\rm MS}$ mass with $\delta m_t \propto m_t$ is appropriate for the hard functions. In the jet function $J_{B,\tau_2}^{(5)}$ one has to adopt a scheme such as MSR [6] with $\delta m_t \sim R \sim \Gamma_t$ to maintain the power counting in the peak region. The MSR scheme is defined by ($a \equiv \alpha_s^{(5)}(R)/4\pi$)

$$m_t^{\rm pole} - m_t^{\rm MSR}(R) \;\equiv\; R\,(\,c_1 a + c_2 a^2 + c_3 a^3 + \dots\,)\,, \tag{4}$$

where $c_1 = 5.333$, $c_2 = 131.785$, $c_3 = 4699.703, \dots$ are precisely the coefficients that define the series relating the $\overline{\rm MS}$ to pole mass, $m_t^{\rm pole} - \overline{m}_t(\overline{m}_t)$ with $R = \overline{m}_t(\overline{m}_t)$. The evolution of the MSR mass with R is also described by R-evolution. The MSR mass is convenient as it is directly related to the $\overline{\rm MS}$ mass, $m_t^{\rm MSR}(\overline{m}_t) = \overline{m}_t(\overline{m}_t)$. Due to $\lim_{R\to 0} m_t^{\rm MSR}(R) = m_t^{\rm pole}$ it interpolates to the pole mass. However, in taking this limit one encounters the Landau singularity reflecting the pole mass renormalon problem.

To sum large logarithms we use τ_2-dependent scales $\mu_i(\tau_2)$ and $R_i(\tau_2)$, known as profile functions [20, 21]. They have canonical scaling in resummation regions, freeze at a perturbative scale to avoid the Landau pole, and exhibit smooth transitions between regions. They are expressed in terms of 9 parameters which are varied to estimate perturbative uncertainties. We develop a natural generalization of those used for massless event shapes in [32], to which they reduce in the massless limit [19].

For a given center of mass energy Q, the key parameters that enter the QCD factorization predictions for the τ_2 distribution are the top mass m_t, the top width Γ_t, the hadronic parameters Ω_i, and the strong coupling $\alpha_s(m_Z)$. We will consider fits both in the pole and the MSR mass schemes. Our results in the MSR scheme are given in terms of $m_t^{\rm MSR}(1\,\mathrm{GeV})$ following [4, 5].

Fit Procedure: For a given $m_t^{\rm MC}$ we produce MC datasets for $\mathrm{d}\sigma/\mathrm{d}\tau_2$ in the peak region for various Q val-

ues. For a given profile and value of $\alpha_s(m_Z)$ we fit the parameters m_t and Ω_i of the hadron level QCD predictions to this MC dataset. We fit for integrals over bins in τ_2 of size $\simeq 0.13\,\text{GeV}/Q$. For each Q value the distribution is normalized over the fit range, and multiple Qs are needed simultaneously to break degeneracies. This procedure is carried out for the MC output and the QCD predictions. We then construct the χ^2 using the statistical uncertainties in the MC datasets. We do the fit by first, for a given value of m_t, minimizing χ^2 with respect to the Ω_i parameters. The resulting marginalized χ^2 is then minimized with respect to m_t used in the QCD predictions. Uncertainties obtained for the QCD parameters from this χ^2 simply reflect the MC statistical uncertainties used to construct the χ^2. When fitting for m_t^{pole} or $m_t^{\text{MSR}}(1\,\text{GeV})$ we find that the resulting χ^2 is no longer sensitive to $\alpha_s(m_Z)$. Therefore we fix $\alpha_s(m_Z)$ to the world average, and do not consider it as a fit parameter.

To estimate the perturbative uncertainty in the QCD predictions we take 500 random points in the profile-function parameter space and perform a fit for each of them. The 500 sets of best-fit values provide an ensemble from which we remove the upper and lower 1.5% in the mass values to eliminate potential numerical outliers. From the ensemble we determine central values from the average of the largest and smallest values and perturbative uncertainties from half the covered interval.

To illustrate the calibration procedure we use Pythia 8.205 [33, 34] with the e^+e^- default tune 7 (the Monash 2013 tune [35] for which $\Lambda_c = 0.5\,\text{GeV}$) for top mass parameter values $m_t^{\text{MC}} = 170$, 171, 172, 173, 174 and 175 GeV. We use a fixed top quark width $\Gamma_t = 1.4\,\text{GeV}$ which is independent of m_t^{MC}. (Final calibration results for a m_t^{MC}-dependent top width differ by less than 25 MeV). No other changes are made to the default settings. To minimize statistical uncertainties we generate each distribution with 10^7 events. We have carried out fits for the following seven Q sets (in GeV units): $(600, 1000, 1400)$, $(700, 1000, 1400)$, $(800, 1000, 1400)$, $(600 - 900)$, $(600 - 1400)$, $(700 - 1000)$ and $(700 - 1400)$, where the ranges refer to steps of 100. For each one of these sets we have considered three ranges of τ_2 in the peak region: $(60\%, 80\%)$, $(70\%, 80\%)$ and $(80\%, 80\%)$, where $(x\%, y\%)$ means that we include regions of the spectra whose $\tau_2 < \tau_2^{\text{peak}}$ having cross-section values larger than $x\%$ of the peak height, and $\tau_2 > \tau_2^{\text{peak}}$ with cross sections larger than $y\%$ of the peak height, where τ_2^{peak} is the peak position. This makes a total of 21 fit settings each of which gives central values and scale uncertainties for the top mass and the Ω_i.

Numerical Results of the Calibration: To visualize the stability of our fits we display in Fig. 1 the distribution of best-fit mass values obtained for 500 random profile functions for $m_t^{\text{MC}} = 173\,\text{GeV}$ based on the Q set $(600 - 1400)$ and the bin range $(60\%, 80\%)$. Results are shown for $m_t^{\text{MSR}}(1\,\text{GeV})$ and m_t^{pole} at NLL and N^{2}LL order, exhibiting good convergence, with the higher order result having a smaller perturbative scale uncertainty. The results for $m_t^{\text{MSR}}(1\,\text{GeV})$ are stable and about 200 MeV below m_t^{MC} confirming the close relation of $m_t^{\text{MSR}}(1\,\text{GeV})$ and m_t^{MC} suggested in Refs. [4, 5]. We observe that m_t^{pole} is about 1.1 GeV (NLL) and 0.7 GeV (N^{2}LL) lower than m_t^{MC}, demonstrating that corrections here are bigger, and *that the MC mass can not simply be identified with the pole mass.* These fit results are compatible with converting m_t^{MSR} with $R \simeq \mu_B \simeq \mu_S Q/m_t \simeq 10\,\text{GeV}$ to m_t^{pole} using Eq. (4), where μ_B is the renormalization scale of the jet function J_{B,τ_2} which governs the dominant mass sensitivity. In Fig. 2 we see the level of agreement between the MC and theory results in the MSR scheme at N^{2}LL order for this fit. The bands show the N^{2}LL perturbative uncertainty from the profile variations.

The results from the fits to the 21 different Q sets and bin ranges mentioned above are quite similar. The differences can be associated to the level of incompatibility of the MC event generator results to the QCD predictions, and unlike the perturbative uncertainties these differences need not necessarily decrease when going from NLL to N^{2}LL. We will use the differences from the 21

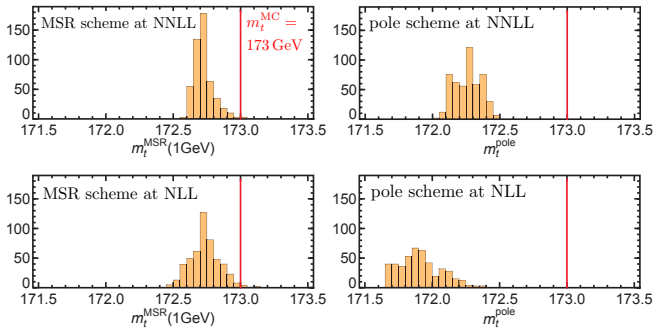

FIG. 1. Distribution of best-fit mass values from the scan over parameters describing perturbative uncertainties. Results are shown for cross sections employing the MSR mass $m_t^{\text{MSR}}(1\,\text{GeV})$ (top two panels) and the pole mass m_t^{pole} (bottom two panels), both at N^{2}LL and NLL. The Pythia datasets use $m_t^{\text{MC}} = 173\,\text{GeV}$ as an input (vertical red lines).

$m_t^{\text{MC}} = 173\,\text{GeV}$ $\left(\tau_2^{e^+e^-}\right)$

mass	order	central	perturb.	incompatibility	total
$m_{t,1\,\text{GeV}}^{\text{MSR}}$	NLL	172.80	0.26	0.14	0.29
$m_{t,1\,\text{GeV}}^{\text{MSR}}$	N^{2}LL	172.82	0.19	0.11	0.22
m_t^{pole}	NLL	172.10	0.34	0.16	0.38
m_t^{pole}	N^{2}LL	172.43	0.18	0.22	0.28

TABLE I. Results of the calibration for $m_t^{\text{MC}} = 173\,\text{GeV}$ in Pythia, combining results from all Q sets and bin ranges. Shown are central values, perturbative and incompatibility uncertainties, and the total uncertainty, all in GeV.

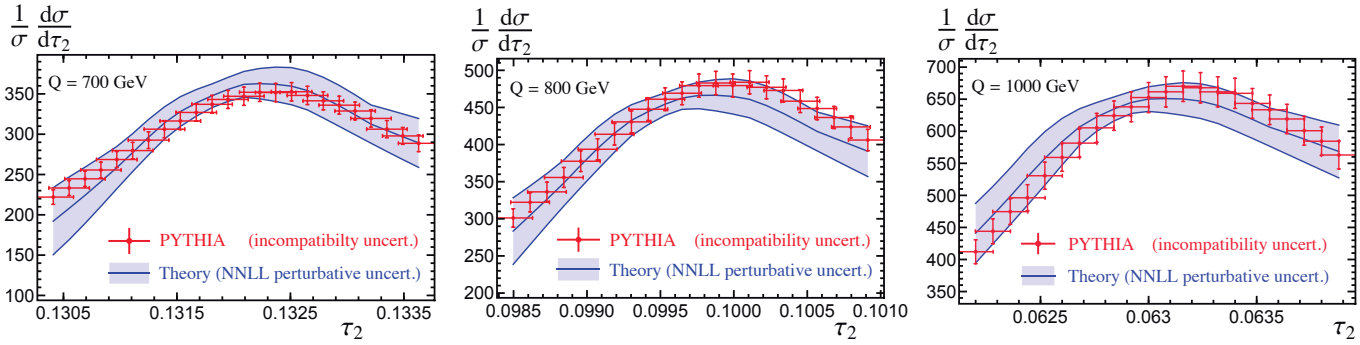

FIG. 2. Comparison of PYTHIA samples with 10^7 events and $m_t^{\rm MC} = 173$ GeV (red dots) to the theoretical prediction in the MSR scheme at N^{2}LL for $m_t^{\rm MSR}(1\text{ GeV}) = 172.81\,\text{GeV}$ and $\Omega_1 = 0.44\,\text{GeV}$. The blue band shows the perturbative uncertainty from a random scan over 500 profile functions. Vertical error bars on the PYTHIA points are obtained by a global rescaling of PYTHIA statistical uncertainties such that the average $\chi^2_{\rm min}/{\rm dof} = 1$ and roughly indicate the incompatibility uncertainties on the cross sections. Horizontal error bars are related to the N^{2}LL incompatibility uncertainty in the MSR mass shown in Tab. I.

fits to assign an additional *incompatibility uncertainty* between QCD and the MC generator for the calibration.

To quote final results we use the following procedure: (1) Take the average of the highest and lowest central values from the 21 sets as the final central value of our calibration. (2) Take the average of the scale uncertainties of these sets as our final estimate for the perturbative uncertainty. (3) Take the half of the difference of the largest and smallest central values from the sets as the incompatibility uncertainty between QCD and the MC. (4) Quadratically add the perturbative, and incompatibility errors to obtain a final uncertainty.

Using α_s values within the uncertainty of the world average $\alpha_s(m_Z) = 0.1181(13)$ gives an additional parametric uncertainty of $\simeq 20\,\text{MeV}$ for $m_t^{\rm MSR}(1\,\text{GeV})$ and $m_t^{\rm pole}$ at N^{2}LL order. This is an order of magnitude smaller than the other uncertainties and we therefore neglect it.

Table I shows our final results for the MSR mass $m_t^{\rm MSR}(1\,\text{GeV})$ and $m_t^{\rm pole}$ at NLL and N^{2}LL order, utilizing the $m_t^{\rm MC} = 173\,\text{GeV}$ dataset. For $m_t^{\rm MSR}(1\,\text{GeV})$ we observe a reduction of perturbative uncertainties from 260 MeV at NLL to 190 MeV at N^{2}LL. The corresponding incompatibility uncertainties are 140 and 110 MeV. The corresponding fit results for the first shape function moment are $\Omega_1^{\rm PY} = 0.42 \pm 0.07 \pm 0.03\,\text{GeV}$ at N^{2}LL and $\Omega_1^{\rm PY} = 0.41 \pm 0.07 \pm 0.02\,\text{GeV}$ at NLL order with the first uncertainty coming from scale variation and second from incompatibility. The result agrees nicely with the expectation that $\Omega_1 \sim \Lambda_{\rm QCD}$. For $m_t^{\rm pole}$ there is a significant difference to $m_t^{\rm MC}$, and we observe that the central value shifts by 330 MeV between NLL and N^{2}LL order. There is a reduction of perturbative uncertainties like in the MSR scheme, however the incompatibility uncertainty increases at N^{2}LL order. These results may not be unexpected, since the pole mass often leads to poor convergence of perturbative series.

Figure 3, shows the outcome of our fits for the MSR mass $m_t^{\rm MSR}(1\,\text{GeV})$ at N^{2}LL order with six different input values for $m_t^{\rm MC}$, and error bars with the total uncertainties. We see the expected strong correlation between these masses. This calibration results in Tab. I and Fig. 3 should be independently determined for each MC and generator setting (such as different tunes).

To the extent that the treatment of the top in MC generators and QCD factorizes for different kinematically sensitive observables and from whether one considers e^+e^- or pp collisions, our method can be used to calibrate $m_t^{\rm MC}$ in current experimental reconstruction analyses. pp collisions introduce initial state radiation, color reconnection, and additional hadronization and multiparton interaction effects, not present in e^+e^-. In the future our method can be extended to use other e^+e^- and also pp observables to directly study these effects and also the universality of the calibration procedure. Prior to this, we believe that applying our e^+e^- calibration to $m_t^{\rm MC}$ from a typical pp reconstruction analysis will give a more accurate result than assuming $m_t^{\rm MC} = m_t^{\rm pole}$. When corresponding hadron level predictions exist, this calibration procedure can also be applied to other MC parameters. The calibration procedure may also provide new ways to test and improve MC event generators.

Acknowledgment: We thank Marcel Vos, Peter Skands, Torbjörn Sjöstrand, Juan Fuster and Frank Tackmann for numerous discussions. We acknowledge partial support by the FWF Austrian Science Fund under the Doctoral Program No. W1252-N27 and the Project No. P28535-N27, the Spanish MINECO Ramón y Cajal program (RYC-2014-16022), the U.S. Department of Energy under the Grant No. DE-SC0011090, and the Simons Foundation through the Grant 327942. We thank the Erwin-Schrödinger International Institute for Mathematics and Physics, the University of Vienna and Cultural Section of the City of Vienna (MA7) for partial support.

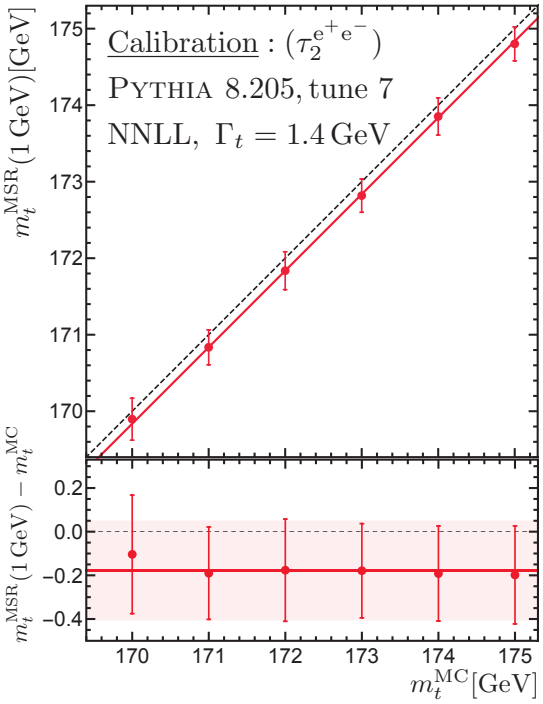

FIG. 3. Dependence of the N^{2}LL fit result for the MSR mass on the input m_t^{MC} value in Pythia. The error bars show the total calibration uncertainty. The red solid lines correspond to the weighted average of the individual results. The red shaded area shows the average of the individual uncertainties.

[1] CDF and D0 (Tevatron Electroweak Working group), (2014), arXiv:1407.2682 [hep-ex].
[2] V. Khachatryan *et al.* (CMS), Phys. Rev. **D93**, 072004 (2016), arXiv:1509.04044 [hep-ex].
[3] M. Aaboud *et al.* (ATLAS), (2016), arXiv:1606.02179 [hep-ex].
[4] A. H. Hoang and I. W. Stewart, *Proceedings, 2nd Workshop on Theory, Phenomenology and Experiments in Heavy Flavour Physics*, Nucl. Phys. Proc. Suppl. **185**, 220 (2008), arXiv:0808.0222 [hep-ph].
[5] A. H. Hoang, in *7th International Workshop on Top Quark Physics (TOP2014) Cannes, France, September 28-October 3, 2014* (2014) arXiv:1412.3649 [hep-ph].
[6] A. H. Hoang, A. Jain, I. Scimemi, and I. W. Stewart, Phys. Rev. Lett. **101**, 151602 (2008), arXiv:0803.4214 [hep-ph].
[7] S. Fleming, A. H. Hoang, S. Mantry, and I. W. Stewart, Phys. Rev. **D77**, 074010 (2008), arXiv:hep-ph/0703207.
[8] S. Fleming, A. H. Hoang, S. Mantry, and I. W. Stewart, Phys. Rev. **D77**, 114003 (2008), arXiv:0711.2079 [hep-ph].
[9] I. W. Stewart, F. J. Tackmann, and W. J. Waalewijn, Phys.Rev.Lett. **105**, 092002 (2010), arXiv:1004.2489 [hep-ph].
[10] G. P. Korchemsky and G. Sterman, Nucl. Phys. **B555**, 335 (1999), arXiv:hep-ph/9902341.
[11] C. W. Bauer, S. Fleming, and M. E. Luke, Phys. Rev. **D63**, 014006 (2001), hep-ph/0005275.
[12] C. W. Bauer, S. Fleming, D. Pirjol, and I. W. Stewart, Phys. Rev. D **63**, 114020 (2001), hep-ph/0011336.
[13] C. W. Bauer and I. W. Stewart, Phys. Lett. B **516**, 134 (2001), hep-ph/0107001.
[14] C. W. Bauer, D. Pirjol, and I. W. Stewart, Phys. Rev. **D65**, 054022 (2002), arXiv:hep-ph/0109045.
[15] A. H. Hoang, A. Pathak, P. Pietrulewicz, and I. W. Stewart, JHEP **12**, 059 (2015), arXiv:1508.04137 [hep-ph].
[16] A. Jain, I. Scimemi, and I. W. Stewart, Phys. Rev. **D77**, 094008 (2008), arXiv:0801.0743 [hep-ph].
[17] S. Gritschacher, A. H. Hoang, I. Jemos, and P. Pietrulewicz, Phys. Rev. **D88**, 034021 (2013), arXiv:1302.4743 [hep-ph].
[18] P. Pietrulewicz, S. Gritschacher, A. H. Hoang, I. Jemos, and V. Mateu, Phys. Rev. **D90**, 114001 (2014), arXiv:1405.4860 [hep-ph].
[19] B. Dehnadi, *Heavy Quark Mass Determinations with Sum Rules and Jets*, Ph.D. thesis, University of Vienna, June (2016).
[20] Z. Ligeti, I. W. Stewart, and F. J. Tackmann, Phys. Rev. **D78**, 114014 (2008), arXiv:0807.1926 [hep-ph].
[21] R. Abbate, M. Fickinger, A. H. Hoang, V. Mateu, and I. W. Stewart, Phys. Rev. **D83**, 074021 (2011), arXiv:1006.3080.
[22] R. Abbate, M. Fickinger, A. H. Hoang, V. Mateu, and I. W. Stewart, Phys. Rev. **D86**, 094002 (2012), arXiv:1204.5746 [hep-ph].
[23] T. Becher and M. D. Schwartz, JHEP **07**, 034 (2008), arXiv:0803.0342 [hep-ph].
[24] R. A. Davison and B. R. Webber, Eur. Phys. J. **C59**, 13 (2009), arXiv:0809.3326 [hep-ph].
[25] T. Gehrmann, M. Jaquier, and G. Luisoni, Eur. Phys. J. **C67**, 57 (2010), arXiv:0911.2422 [hep-ph].
[26] Y.-T. Chien and M. D. Schwartz, JHEP **08**, 058 (2010), arXiv:1005.1644 [hep-ph].
[27] T. Gehrmann, G. Luisoni, and P. F. Monni, Eur. Phys. J. **C73**, 2265 (2013), arXiv:1210.6945 [hep-ph].
[28] A. H. Hoang, D. W. Kolodrubetz, V. Mateu, and I. W. Stewart, Phys. Rev. **D91**, 094018 (2015), arXiv:1501.04111 [hep-ph].
[29] A. H. Hoang and I. W. Stewart, Phys. Lett. **B660**, 483 (2008), arXiv:0709.3519 [hep-ph].
[30] A. H. Hoang and S. Kluth, (2008), arXiv:0806.3852 [hep-ph].
[31] A. H. Hoang, A. Jain, I. Scimemi, and I. W. Stewart, Phys. Rev. **D82**, 011501 (2010), arXiv:0908.3189 [hep-ph].
[32] A. H. Hoang, D. W. Kolodrubetz, V. Mateu, and I. W. Stewart, Phys. Rev. **D91**, 094017 (2015), arXiv:1411.6633 [hep-ph].
[33] T. Sjöstrand, S. Mrenna, and P. Z. Skands, JHEP **05**, 026 (2006), arXiv:hep-ph/0603175 [hep-ph].
[34] T. Sjöstrand, S. Ask, J. R. Christiansen, R. Corke, N. Desai, P. Ilten, S. Mrenna, S. Prestel, C. O. Rasmussen, and P. Z. Skands, Comput. Phys. Commun. **191**, 159 (2015), arXiv:1410.3012 [hep-ph].
[35] P. Skands, S. Carrazza, and J. Rojo, Eur. Phys. J. **C74**, 3024 (2014), arXiv:1404.5630 [hep-ph].